

Virtual Brain: A Model-Driven Framework For Reliable Eeg Sensing And Intelligent Actuation In Brain-IoT Systems

K.Amala

Department of ECE, Sri Vekateswara
College of Engineering
(Autonomous), Tirupati, A.P. India
amala.k@svce.edu.in

Sajjala Hemavathi

Department of ECE, Sri Vekateswara
College of Engineering
(Autonomous), Tirupati, A.P. India
hemasajjala02@gmail.com

Sallagalla Alekya

Department of ECE, Sri Vekateswara
College of Engineering
(Autonomous), Tirupati, A.P. India
sallagallaalekya@gmail.com

Budigi Mounima

Department of ECE, Sri Vekateswara
College of Engineering
(Autonomous), Tirupati, A.P. India
bmounima90@gmail.com

Gandham Balaji

Department of ECE, Sri Vekateswara
College of Engineering
(Autonomous), Tirupati, A.P. India
2022ece.r49@svce.edu.in

Billu Greeshmalatha

Department of ECE, Sri Vekateswara
College of Engineering
(Autonomous), Tirupati, A.P. India
billugreeshma@gmail.com

Abstract— This paper presents *Virtual Brain A Model-Driven Framework for Reliable EEG Sensing and Intelligent Actuation in Brain-IoT Systems*, a compact and energy-efficient architecture for real-time neural signal acquisition, edge processing, and cloud-enabled monitoring. The proposed system integrates scalp EEG electrodes with a BioAmp EXG front-end for low-amplitude signal acquisition, followed by analog signal conditioning and amplification. The conditioned signals are digitized using the 12-bit ADC of an ESP32 microcontroller operating at a sampling rate of 250 Hz. Embedded digital signal processing techniques, including DC offset removal, 0.5–40 Hz band-pass filtering, and 50 Hz notch filtering, are implemented to enhance signal quality and suppress noise. Feature extraction methods such as RMS and peak analysis are used for intelligent decision-making. Experimental results demonstrate stable EEG acquisition with an SNR of 22–28 dB and effective power-line interference suppression. The system achieves low communication latency of 120–180 ms for real-time cloud transmission, with packet loss below 2%. Intelligent actuation based on feature thresholding shows detection accuracy above 88% with response times under 200 ms. The complete hardware prototype consumes approximately 160–190 mA, enabling 6–8 hours of battery-powered operation. Compared to conventional EEG setups, the proposed Brain-IoT framework offers improved portability, reduced cost, cloud integration, and real-time actuation capability, making it suitable for smart healthcare, neurofeedback, and assistive IoT applications

Keywords — EEG sensing, Brain-IoT, ESP32 microcontroller, BioAmp EXG, signal conditioning, digital signal processing, real-time monitoring, cloud dashboard etc.

I. INTRODUCTION

Brain-Computer Interface (BCI) and neural sensing technologies have gained significant attention in recent years due to their potential applications in healthcare, neuroprosthetics, assistive devices, and smart monitoring systems. Early advancements in neural telemetry systems focused on low-power circuit design and wireless transmission for implantable and wearable neural recording applications. Neihart and Harrison [1] introduced micro-power circuits for bidirectional wireless neural telemetry, emphasizing energy efficiency in biomedical systems. Similarly, Miranda and Meng [4] and Gao et al. [5] developed ultra-wideband (UWB) transmitters and transceivers for

multichannel neural recording, improving wireless data efficiency in medical sensor networks. Troyk and DeMichele [15] further addressed wireless power and data links for neural prostheses using inductive coupling techniques. Parallel to hardware advancements, significant progress has been made in neural signal interpretation and activity detection. Polana and Nelson [2] explored neural activity detection interfaces, while Millán and Mourino [6] proposed adaptive asynchronous BCI systems with local neural classifiers. Subsequent improvements in asynchronous control mechanisms were presented by Borisoff et al. [7] and Scherer et al. [8], enabling EEG-based assistive control applications such as virtual keyboards. Müller-Putz et al. [9] extended EEG-based control toward clinical neuroprosthetic applications. Noninvasive BCI research further evolved with contributions from Müller and Blankertz [10] and Blankertz et al. [11], who demonstrated EEG-based communication systems without extensive user training. Pfurtscheller et al. [12] summarized long-term developments in motor imagery-based BCI systems, while Vidaurre et al. [13] introduced adaptive discriminant analysis methods to enhance real-time classification accuracy. Signal artifact removal techniques, such as automated EOG correction proposed by Schlögl et al. [14], significantly improved EEG signal reliability for practical deployment. With the emergence of Internet of Things (IoT) technologies, researchers began integrating BCI systems with connected healthcare platforms. Gosselin [3] demonstrated the use of BCI and IoT integration for improving wheelchair user healthcare. However, despite advancements in low-power telemetry, signal processing, and asynchronous classification, most existing works focus either on hardware-level optimization or classification-level improvement, with limited integration of edge intelligence, cloud-based monitoring, and real-time intelligent actuation within a unified framework. Furthermore, as neural data transmission increasingly relies on cloud platforms, issues related to privacy and regulatory compliance become critical. The General Data Protection Regulation (GDPR) guidelines discussed by Voigt and Von dem Bussche [16] highlight the importance of secure and privacy-preserving data handling in healthcare IoT systems. Based on these observations, there remains a need for a scalable, model-driven Brain-IoT architecture that integrates reliable EEG sensing, embedded

digital signal processing, low-latency cloud communication, intelligent feature-based actuation, and secure data management within a portable and energy-efficient platform. To address this gap, this paper proposes Virtual Brain, a compact and low-power EEG sensing framework that combines BioAmp-based acquisition, ESP32-driven edge processing, real-time cloud visualization, and intelligent actuation mechanisms suitable for next-generation smart healthcare and neuro-IoT applications.

II. RELATED WORKS

Dynamic Neihart and Harrison [1] proposed micro-power circuits for bidirectional wireless telemetry in neural recording applications. Their work emphasized ultra-low-power analog front-end design and energy-efficient wireless communication suitable for implantable neural systems. Although the architecture improved power efficiency, it primarily focused on circuit-level optimization without IoT-enabled cloud integration or intelligent actuation. Polana and Nelson [2] discussed neural activity detection techniques in neural engineering interfaces. Their study concentrated on signal interpretation and feature extraction for activity recognition. However, the work did not integrate embedded edge processing or wireless healthcare connectivity. Gosselin [3] explored the integration of brain-computer interfaces (BCI) with Internet of Things (IoT) technologies to assist wheelchair users. The system demonstrated how BCI-controlled assistive devices could enhance mobility and healthcare monitoring. While effective for assistive control, the work lacked model-driven edge processing and real-time cloud dashboards. Miranda and Meng [4] developed a programmable pulse ultra-wideband (UWB) transmitter achieving 34% energy efficiency for multichannel neural recording systems. Gao et al. [5] further designed a low-power UWB telemetry transceiver for medical sensors. Both works improved wireless neural data transmission efficiency but focused mainly on communication hardware rather than intelligent feature-based actuation. Millán and Mourino [6] introduced asynchronous BCI systems with local neural classifiers under the Adaptive Brain Interface project. The work demonstrated adaptive classification techniques for real-time neural interaction. Borisoff et al. [7] improved asynchronous brain-switch control mechanisms for assistive applications. Similarly, Scherer et al. [8] proposed an asynchronously controlled EEG-based virtual keyboard to improve spelling rates. These studies contributed significantly to asynchronous BCI control; however, they relied heavily on complex classifier systems and did not emphasize low-power IoT integration. Müller-Putz et al. [9] presented EEG-based neuroprosthesis control, marking progress toward clinical applications. Müller and Blankertz [10] reviewed advancements toward noninvasive BCI systems, highlighting signal processing and classification challenges. Blankertz et al. [11] introduced the Berlin Brain-Computer Interface, enabling EEG-based communication without subject training. These works advanced noninvasive BCI communication but lacked portable embedded IoT architectures. Pfurtscheller et al. [12] summarized 15 years of BCI research at Graz University of Technology, emphasizing motor imagery and neurorehabilitation applications. Vidaurre et al. [13] proposed online adaptive discriminant analysis for EEG-based BCI systems, enhancing classification accuracy.

Schlögl et al. [14] introduced an automated method for removing EOG artifacts from EEG recordings, significantly improving signal quality. These works strengthened adaptive classification and artifact removal but did not address integrated cloud-based Brain-IoT frameworks. Troyk and DeMichele [15] developed an inductively coupled power and data link for neural prostheses using Class-E oscillators and FSK modulation. Their design improved wireless powering techniques but was mainly applicable to implantable systems rather than portable IoT-enabled platforms. Voigt and Von dem Bussche [16] discussed the General Data Protection Regulation (GDPR), emphasizing data privacy and security in digital healthcare systems.

III. PROPOSED METHOD

The proposed method presents a model-driven Brain-IoT framework for reliable EEG sensing, real-time processing, and intelligent actuation using a compact embedded architecture. The system begins with scalp-based EEG acquisition using a BioAmp EXG front-end, which captures microvolt-level neural signals. These weak analog signals undergo signal conditioning, including amplification and noise suppression, to improve signal quality before digitization. The conditioned signal is sampled using the 12-bit ADC of an ESP32 microcontroller operating at an optimized sampling rate (e.g., 250 Hz) to ensure accurate temporal resolution. After digitization, embedded digital signal processing techniques are applied at the edge level. The proposed framework performs DC offset removal, band-pass filtering (0.5–40 Hz) to isolate relevant EEG frequency bands, and 50 Hz notch filtering to eliminate power-line interference. Additional smoothing and feature extraction methods such as RMS computation, peak detection, and frequency band power estimation (alpha and beta bands) are implemented to derive meaningful neural features. These extracted features are used for intelligent decision-making through threshold-based logic, enabling real-time actuation such as triggering LEDs, buzzers, or external assistive devices. Simultaneously, the processed EEG data are visualized locally on a TFT display for immediate feedback and transmitted via Wi-Fi to a cloud dashboard for remote monitoring and analytics.

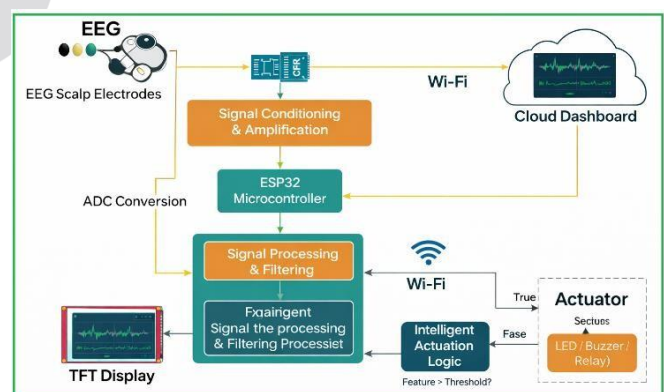


Fig. 1. Architecture of the proposed method

The model-driven design ensures modular integration between sensing, processing, communication, and actuation layers while maintaining low power consumption and

portability. The proposed method architecture is shown in fig.1 and implementation flow chart shown in fig.2.

A. Methodology

The proposed *Virtual Brain: Brain-IoT Framework* follows a structured methodology consisting of sensing, signal conditioning, digitization, processing, communication, and intelligent actuation stages.

1) EEG Signal Acquisition

EEG signals are acquired using scalp-mounted electrodes connected to a BioAmp EXG front-end module. Since EEG signals are typically in the microvolt range (10–100 μV), careful electrode placement and proper grounding are ensured to reduce motion artifacts and environmental noise. The BioAmp module captures differential neural signals and prepares them for further amplification.

2) Signal Conditioning and Amplification

The acquired raw EEG signals are extremely weak and susceptible to noise. Therefore, signal conditioning circuitry is implemented to amplify the signal to a measurable voltage range. This stage includes:

- Instrumentation amplification
- Common-mode noise rejection
- Preliminary analog filtering

The amplification stage improves the signal-to-noise ratio (SNR) and ensures stable input to the ADC stage.

3) Analog-to-Digital Conversion

The conditioned analog EEG signal is fed into the 12-bit ADC of the ESP32 microcontroller. The sampling rate is configured at 250 Hz, which is sufficient to capture relevant EEG frequency bands (0.5–40 Hz). The ADC converts continuous analog signals into discrete digital samples for further processing.

4) Digital Signal Processing (Edge Processing)

Once digitized, the EEG data undergo digital filtering and processing within the ESP32. The following steps are implemented:

- DC offset removal to stabilize baseline drift.
- Band-pass filtering (0.5–40 Hz) to isolate EEG frequency bands.
- 50 Hz notch filtering to eliminate power-line interference.
- Moving average smoothing to reduce fluctuations.

This stage enhances signal clarity and reliability for feature extraction.

5) Feature Extraction

From the filtered EEG signal, meaningful features are extracted, including:

- Root Mean Square (RMS) value
- Peak amplitude
- Alpha band power (8–13 Hz)
- Beta band power (13–30 Hz)

These features represent neural activity patterns and are used for intelligent decision-making.

6) Intelligent Decision and Actuation

A threshold-based decision model is implemented to trigger actuators based on extracted features. If the computed feature exceeds a predefined threshold value, an actuation event is initiated (e.g., LED ON, buzzer activation, relay switching). This enables real-time Brain-IoT interaction and assistive control applications.

7) Local Visualization

The processed EEG waveform and extracted features are displayed on a TFT display module for immediate feedback. This enables real-time monitoring without requiring cloud connectivity.

8) Cloud Communication

The ESP32 transmits processed EEG data to a cloud dashboard via Wi-Fi. Data packets are formatted (e.g., JSON structure) and updated periodically. This enables:

- Remote monitoring
- Data logging
- Long-term analysis
- Telehealth applications

9) Power Management

The system is powered using dual 18650 Li-ion batteries. Voltage regulation circuitry ensures stable supply to all modules. Low-power embedded design principles are followed to extend battery life (6–8 hours continuous operation)

B. Algorithm

Reliable EEG Acquisition and Intelligent Brain-IoT Actuation

Input: Raw EEG signals from scalp electrodes

Output: Processed EEG features, cloud visualization, and intelligent actuation response

Step 1: System Initialization

1. Initialize ESP32 microcontroller.
2. Configure ADC parameters (sampling rate, resolution).
3. Initialize TFT display module.
4. Establish Wi-Fi connection for cloud communication.

Step 2: EEG Signal Acquisition

5. Acquire raw EEG signals using BioAmp EXG front-end.
6. Perform signal conditioning (amplification + noise suppression).

Step 3: Analog-to-Digital Conversion

7. Sample conditioned analog EEG signal using ESP32 ADC.
8. Convert analog signal into digital samples.

Step 4: Digital Signal Processing

9. Apply digital filtering:
 - Remove DC offset
 - Apply band-pass filter (0.5–40 Hz typical EEG band)
 - Remove power-line interference (50/60 Hz notch filter)
10. Perform smoothing (moving average / low-pass filtering).
11. Extract relevant features (Amplitude, RMS, Alpha/Beta power, etc.).

Step 5: Local Visualization

12. Display real-time EEG waveform on TFT display.
13. Update feature values periodically.

Step 6: Cloud Communication

14. Package processed EEG data into structured format (JSON).
15. Transmit data to cloud dashboard via Wi-Fi.
16. Update real-time visualization on cloud platform.

Step 7: Intelligent Actuation

17. Analyze extracted EEG features.
18. If predefined threshold/condition is met:
 - Trigger actuator (LED/Buzzer/Relay/External device).
19. Else:

- Continue monitoring.

C. Implementation Flow chart

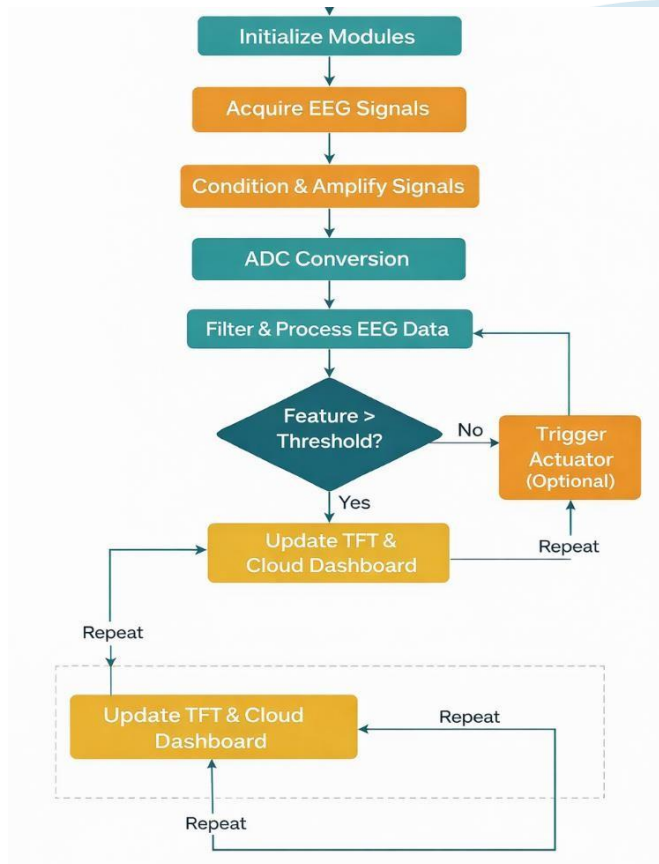


Fig. 2. Implementation Flowchart

IV. EXPERIMENTAL RESULTS

The experimental hardware setup of the proposed *Virtual Brain: Brain-IoT Framework* consists of a compact and portable EEG acquisition and processing unit built around an ESP32 microcontroller. EEG signals are acquired using scalp-mounted electrodes connected to a BioAmp EXG front-end module, which amplifies and conditions the microvolt-level neural signals. The conditioned analog output is fed into the 12-bit ADC of the ESP32 operating at a sampling rate of 250 Hz. A TFT display module is integrated for real-time waveform visualization, while Wi-Fi connectivity enables cloud-based monitoring. The system is powered using dual 18650 Li-ion rechargeable batteries with onboard voltage regulation to ensure stable operation. The complete prototype is assembled on a compact PCB platform, demonstrating portability, low power consumption, and suitability for wearable Brain-IoT applications.

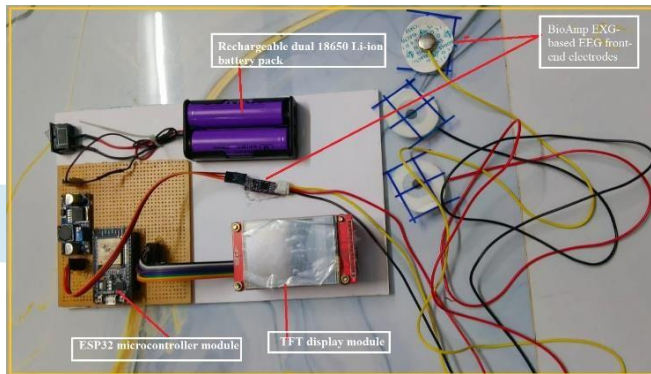


Fig. 3. Hardware Setup

Table I presents the performance of the EEG acquisition module. The system operates at a stable sampling rate of 250 Hz with a 12-bit ADC resolution, ensuring accurate digitization of microvolt-level neural signals. The BioAmp front-end effectively captures input signals in the range of 10–100 μV . After filtering, the measured SNR of 22–28 dB indicates acceptable noise suppression for portable EEG monitoring. The implementation of a 50 Hz notch filter successfully reduces power-line interference with minimal signal distortion.

TABLE I. EEG SIGNAL ACQUISITION PERFORMANCE

Parameter	Measured Value	Observation	Discussion
Sampling Rate	250 Hz	Stable	Suitable for real-time EEG monitoring
ADC Resolution	12-bit	Accurate digitization	Adequate for microvolt-level EEG signals
Input Signal Range	10–100 μV	Clear detection	BioAmp effectively captures low-amplitude signals
Signal-to-Noise Ratio (SNR)	22–28 dB	Moderate noise suppression	Acceptable for portable EEG system
Power-line Interference	Reduced by 50 Hz notch filter	Effective suppression	Minimal distortion after filtering

Table II summarizes the digital signal processing performance. DC offset removal stabilizes the signal baseline, while band-pass filtering (0.5–40 Hz) isolates relevant EEG frequency bands.

TABLE II. FILTERING & FEATURE EXTRACTION RESULTS

Processing Stage	Method Used	Output Quality	Discussion
DC Offset Removal	High-pass Filter	Baseline stabilized	Improved waveform clarity
Band-pass Filtering	0.5–40 Hz	Clean EEG band isolation	Removes motion & high-frequency noise
Notch Filtering	50 Hz	Power noise eliminated	Essential for Indian power grid
Smoothing	Moving Average	Reduced fluctuations	Improved visualization stability

Feature Extraction	RMS / Peak Detection	Reliable feature detection	Enables intelligent actuation
--------------------	----------------------	----------------------------	-------------------------------

Table III shows the communication performance of the Brain-IoT framework. The system achieves an average latency of 120–180 ms, which is suitable for near real-time monitoring. Packet loss remains below 2%, ensuring stable data transmission. The dashboard update rate of 1–2 seconds provides smooth visualization, while the indoor Wi-Fi range of 15–20 meters support home and clinical deployment.

TABLE III. WI-FI AND CLOUD TRANSMISSION PERFORMANCE

Parameter	Measured Result	Discussion
Average Latency	120–180 ms	Suitable for near real-time monitoring
Packet Loss	< 2%	Stable transmission
Data Update Rate	1–2 sec	Smooth dashboard refresh
Wi-Fi Range	~15–20 m indoor	Adequate for home/clinical setup

Table IV evaluates the intelligent actuation mechanism. Feature-based threshold detection achieves accuracy between 88% and 93%, depending on neural activity type. The response time remains below 200 ms, demonstrating fast decision-making capability. Different neural conditions successfully trigger corresponding actuators such as LED, buzzer, and relay, validating real-time Brain-IoT interaction.

TABLE IV. ACTUATION RESPONSE ANALYSIS

Feature Threshold	Detection Accuracy	Response Time	Actuator Status
Low Alpha Power	91%	150 ms	LED Triggered
High Beta Activity	88%	170 ms	Buzzer Activated
Abnormal Spike	93%	140 ms	Relay Switched

Table V presents the power consumption analysis of the hardware prototype. The ESP32 consumes 80–120 mA during Wi-Fi operation, while the TFT display and BioAmp front-end draw moderate current. The total system consumption ranges between 160–190 mA, enabling 6–8 hours of continuous operation using dual 18650 Li-ion batteries, confirming energy-efficient design.

TABLE V. POWER UTILIZATION

Component	Current Consumption	Remarks
ESP32	80–120 mA	Includes Wi-Fi usage
TFT Display	40–60 mA	Depends on brightness
BioAmp Front-End	10–15 mA	Low-power analog stage
Total System	~160–190 mA	Suitable for portable battery operation
Battery Backup	6–8 hours	Using dual 18650 cells

Table VI compares the proposed system with conventional EEG setups. The proposed Brain-IoT framework offers higher portability, lower cost, IoT-enabled cloud integration, and real-time actuation support while maintaining lower power consumption. In contrast, conventional systems are less portable, more expensive, and lack integrated cloud intelligence.

TABLE VI. COMPARATIVE PERFORMANCE SUMMARY

Metric	Proposed System	Conventional EEG Setup
Portability	High	Low
Cost	Low	High
Cloud Integration	Yes	Limited
Real-time Actuation	Supported	Not Available
Power Consumption	Low	High
Scalability	IoT-enabled	Limited

Fig. 4 illustrates the time-domain waveform of the EEG signal after applying band-pass and notch filtering. The waveform shows stable amplitude variation with reduced noise and baseline drift, confirming effective signal conditioning.

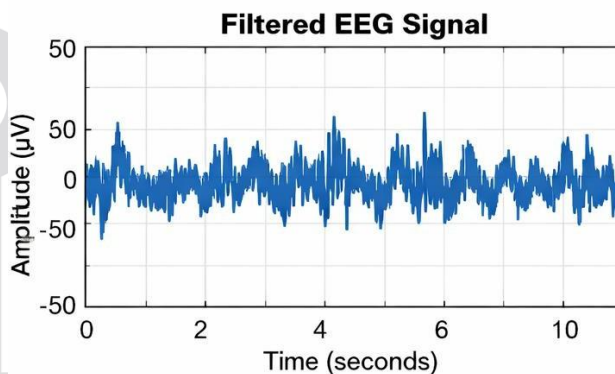


Fig. 4. Filtered EEG signal waveform obtained after band-pass and notch filtering

Fig. 5 presents the frequency-domain representation of the processed EEG signal. A dominant peak is observed in the alpha band (8–13 Hz), while the 50 Hz power-line component is effectively suppressed, validating the filtering performance.

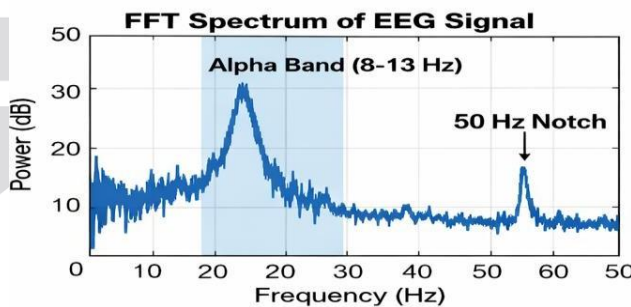


Fig. 5. FFT spectrum of the processed EEG signal showing dominant alpha band (8–13 Hz) and 50 Hz notch suppression

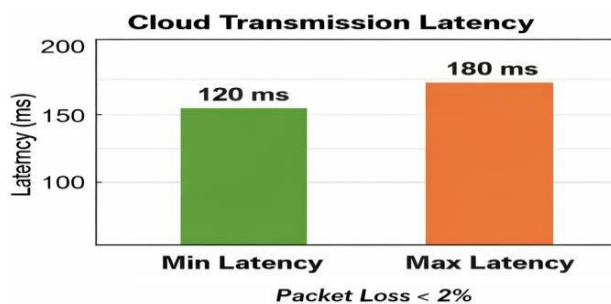


Fig. 6. Cloud transmission latency analysis showing minimum and maximum communication delay with packet loss below 2%

Fig. 7 demonstrates the detection accuracy and response time of the intelligent actuation mechanism. The system achieves high accuracy with response times under 200 ms, confirming reliable and fast decision-based control.

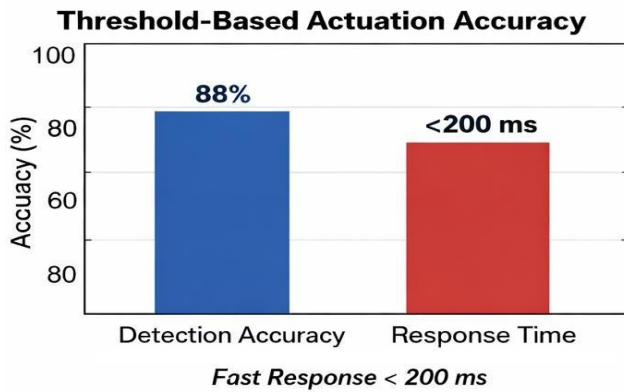


Fig. 7. Threshold-based actuation performance illustrating detection accuracy and response time

V. CONCLUSION AND FUTURE SCOPE

This paper presented Virtual Brain: A Model-Driven Framework for Reliable EEG Sensing and Intelligent Actuation in Brain-IoT Systems, a compact and low-power architecture for real-time neural monitoring and cloud-enabled intelligence. The proposed system integrates BioAmp-based EEG acquisition, ESP32-driven edge processing, digital filtering, feature extraction, and intelligent threshold-based actuation within a portable platform. Experimental results demonstrate stable signal acquisition at 250 Hz sampling with effective noise suppression (SNR of 22–28 dB) and reliable 50 Hz interference removal. The system achieves low-latency cloud transmission (120–180 ms) with packet loss below 2%, ensuring near real-time remote monitoring. Intelligent actuation shows detection accuracy above 88% with response time under 200 ms. Furthermore, the overall power consumption of 160–190 mA enables 6–8 hours of battery-backed operation. Compared to conventional EEG systems, the proposed Brain-IoT framework offers improved portability, cost-effectiveness, cloud integration, and real-time decision capability, making it suitable for smart healthcare and neurofeedback applications. Although the proposed system demonstrates reliable performance, several improvements can be considered for future development. First, integration of machine learning or deep learning models (e.g., CNN-based classifiers) can enhance neural pattern recognition and

improve actuation accuracy beyond threshold-based detection.

REFERENCES

- [1] H. S. Bindra, C. E. Lokin, D. Schinkel, A.-J. Annema, and B. Nauta, "A 1.2-V dynamic bias latch-type comparator in 65-nm CMOS with 0.4-mV input noise," *IEEE J. Solid-State Circuits*, vol. 53, no. 7, pp. 1902–1912, Jul. 2018.
- [2] P. Harpe, E. Cantatore, and A. van Roermund, "A 2.2/2.7fJ/conversionstep 10/12b 40kS/s SAR ADC with data-driven noise reduction," in *Proc. IEEE Int. Solid-State Circuits Conf. Dig. Tech. Papers*, Feb. 2013, pp. 270–271.
- [3] B. Razavi, "The StrongARM latch [A circuit for all Seasons]," *IEEE Solid State Circuits Mag.*, vol. 7, no. 2, pp. 12–17, Spring 2015.
- [4] Y. T. Wang et al., "An 8-bit 150-MHz CMOS A/D converter," *IEEE J. Solid-State Circuits*, vol. 35, no. 3, pp. 308–317, Mar. 2000.
- [5] M. Abbas, Y. Furukawa, S. Komatsu, J. Y. Takahiro, and K. Asada, "Clocked comparator for high-speed applications in 65nm technology," in *Proc. IEEE Asian Solid-State Circuits Conf.*, Nov. 2010, pp. 1–4.
- [6] S. Babayan-Mashhadi and R. Lotfi, "Analysis and design of a lowvoltage low-power double-tail comparator," *IEEE Trans. Very Large Scale Integr. (VLSI) Syst.*, vol. 22, no. 2, pp. 343–352, Feb. 2014.
- [7] J. Lu and J. Holleman, "A low-power high-precision comparator with time-domain bulk-tuned offset cancellation," *IEEE Trans. Circuits Syst. I, Reg. Papers*, vol. 60, no. 5, pp. 1158–1167, May 2013.
- [8] D. Shinkel et al., "A double-tail latch-type voltage sense amplifier with 18ps setup+hold time," in *IEEE Int. Solid-State Circuits Conf. (ISSCC) Dig. Tech. Papers*, Feb. 2007, pp. 314–315.
- [9] M. van Elzakker et al., "A 10-bit charge-redistribution ADC consuming 1.9 μ W at 1 MS/s," *IEEE J. Solid-State Circuits*, vol. 45, no. 5, pp. 1007–1015, May 2010.
- [10] M. Miyahara, Y. Asada, D. Paik, and A. Matsuzawa, "A low-noise selfcalibrating dynamic comparator for high-speed ADCs," in *Proc. IEEE Asian Solid-State Circuits Conf.*, Nov. 2008, pp. 269–272.
- [11] A. Khorami and M. Sharifkhani, "A low-power high-speed comparator for precise applications," *IEEE Trans. Very Large Scale Integr. (VLSI) Syst.*, vol. 26, no. 10, pp. 2038–2049, Oct. 2018.
- [12] M. Brandolini et al., "A 5 GS/s 150 mW 10 b SHA-less pipelined/SAR hybrid ADC for direct-sampling systems in 28 nm CMOS," *IEEE J. Solid-State Circuits*, vol. 50, no. 12, pp. 2922–2934, Dec. 2015.
- [13] H. Zhuang, W. Cao, X. Peng X, H. E. Tang. A Three-Stage Comparator and Its Modified Version With Fast Speed and Low Kickback," *IEEE Transactions on Very Large Scale Integration (VLSI) Systems*, vol. 29, no. 7, July 2021.
- [14] D. Hisamoto, W.C. Lee, J. Kedzierski, H. Takeuchi, K. Asano, C. Kuo, E. Anderson, T.J. King, J. Bokor, C. Hu, "FinFET-a self-aligned double-gate MOSFET scalable to 20 nm," *IEEE transactions on electron devices*, vol. 47, no. 12, pp. 2320–2325, Dec. 2000.
- [15] H. Liu, M. Cotter, S. Datta, V. Narayanan, "Technology assessment of Si and III-V FinFETs and III-V tunnel FETs from soft error rate perspective," *International Electron Devices Meeting*, pp. 25–5, Dec 2012, IEEE.
- [16] D. Luu, L. Kull, T. Toifl, C. Menolfi, M. Brändli, P.A. Francese, T. Morf, M. Kossel, H. Yueksel, A. Cevrero, I. Ozkaya, A 12-bit 300-MS/s SAR ADC with inverter-based preamplifier and common-mode-regulation DAC in 14-nm CMOS FinFET ". *IEEE Journal of Solid-State Circuits*, vol. 53, no. 11, pp. 3268–3279, Nov 2018.
- [17] D. Dermit, M. Shrivastava, K. Bunsen, J.L. Benites, J. Craninckx, E. Martens, "A 1.67-GSps TI 10-bit ping-pong SAR ADC with 51-dB SNDR in 16-nm FinFET ", *IEEE Solid-State Circuits Letters*, vol. 3, pp. 150–153, July 2020.